

Spectral Galerkin transfer operator methods in uniformly-expanding dynamics

Caroline Wormell

The University of Sydney

8th July, 2019

Introduction

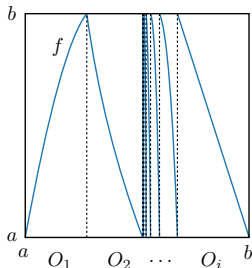
- Interested in ergodic properties of chaotic systems: invariant measures, statistical limit laws, etc.
- Typically these quantities in general do not have explicit solutions: numerics are needed.
- Accurate, fast, transparent numerics that capitalise on smooth structure are important for extending understanding (c.f. PDEs, non-chaotic ODEs. . .)

Goal: powerful numerics for smooth ergodic theory of a useful subclass of chaotic systems.

Chaotic maps

We consider maps of the interval $f : [a, b] \rightarrow [a, b]$ with nice properties:

- Countable partition $\overline{\bigcup_{i \in I} O_i} = [a, b]$,
 $f|_{O_i}$ bijections with inverses v_i
- Regularity conditions
on distortion $D_i := \log |v_i'|$, either:
 - $\sup_{s \leq r, i \in I} \|D_i^{(r)}\|_\infty \leq \infty$ for some r ;
 - D_i have unif. bounded analytic extensions onto an open complex set
- Uniform bound on $d(O_i, \{a, b\})/|O_i|$
for $a, b \notin O_i$. (technical)
- Uniformly C-expanding...



Chaotic maps: Expansion condition

Standard condition is *uniformly expanding*:

$$\inf_{x \in O_i, i \in I} |f'(x)| = \gamma > 1$$

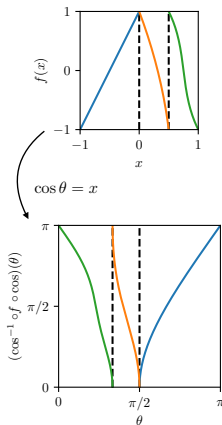
We instead use *C-uniformly expanding*:

$$\inf_{x \in O_i, i \in I} \sqrt{\frac{1-x^2}{1-f(x)^2}} |f'(x)| = \check{\gamma} > 1,$$

where domain $[a, b]$ is rescaled to $[-1, 1]$.

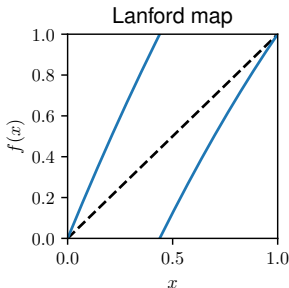
- $\iff \cos^{-1} \circ f \circ \cos$ unif. expanding
- If f is uniformly expanding then some f^n is C-unif. exp. (typically $n = 1$)

Notation: $w_i(\theta) = (\cos^{-1} \circ v_i \circ \cos)(\theta)$,
with $\sup_{i, \theta} |w'_i| = \check{\gamma}^{-1} < 1$.



Examples of maps

- Tupling maps on $[0, 1]$, $f(x) = kx \bmod 1$ for $k = 2, 3, \dots$
- Continued fraction maps, e.g. Gauss map on $[0, 1]$, $f(x) = x^{-1} \bmod 1$, with change of variable $y = 2^x$
- Standard test map for numerics: Lanford map on $[0, 1]$, $f(x) = 2x + \frac{1}{2}x(1 - x) \bmod 1$ (see Figure)



Long-time statistical properties

These maps are chaotic with nice statistical properties. Two we are interested in:

- Absolutely continuous invariant measures (acims) ρ :

$$\frac{1}{N} \sum_{n=0}^{N-1} A(f^n(x_0)) \xrightarrow[\text{Leb.-a.e. } x_0]{N \rightarrow \infty} \int_a^b A \rho \, dx. \quad (*)$$

- Diffusion coefficients: CLT correction to $(*)$ with variance

$$\sigma_f^2(A) = \sum_{n=-\infty}^{\infty} \int_a^b A \circ f^{|n|} \left(A - \int_a^b A \rho \, d\xi \right) dx,$$

well-defined if A is of bounded variation.

Transfer operator

The transfer operator $\mathcal{L} : \mathcal{B} \rightarrow \mathcal{B}$ tracks the action of the map f on signed measure densities in some Banach space \mathcal{B} of smooth functions:

$$\int_a^b A \circ f \varphi \, dx = \int_a^b A \mathcal{L}\varphi \, dx.$$

Has explicit formula for pointwise evaluation:

$$(\mathcal{L}\varphi)(x) = \sum_{i \in I} \sigma_i v_i'(x) \varphi(v_i(x)),$$

where v_i are the inverses of $f|_{O_i}$, and $\sigma_i = \text{sign } v_i'$.

Transfer operator

Statistical quantities of interest can be expressed in terms of linear algebraic properties of the transfer operator:

- Acim ρ satisfies

$$\begin{cases} \mathcal{L}\rho &= \rho, \\ \mathcal{S}\rho &= 1, \end{cases}$$

where $\mathcal{S}\varphi := \int_b^a \varphi \, dx$.

- Diffusion coefficient $\sigma_f^2(A)$ satisfies

$$\sigma_f^2(A) = \mathcal{S} \left[A \sum_{n=-\infty}^{\infty} \mathcal{L}^{|n|} (\rho A - \rho \mathcal{S}[\rho A]) \right]$$

In general, no explicit solutions!

Galerkin method

Take a family of finite-rank projections $\mathcal{P}_n : \mathcal{B} \rightarrow \mathcal{B}$ which asymptotically approximate the identity.

Pick large(ish) n :

- Compute the finite-dimensional operator $\mathcal{L}_n := \mathcal{P}_n \mathcal{L} \mathcal{P}_n|_{\text{im } \mathcal{P}_n}$.
- Substitute $\mathcal{P}_n \mathcal{L} \mathcal{P}_n|_{\text{im } \mathcal{P}_n}$ for \mathcal{L} in the problem of interest, e.g. for acim $\mathcal{P}_n \mathcal{L} \rho_n = \rho_n$.
- Numerically solve to get estimate: e.g. ρ_n should approximate true acim ρ .

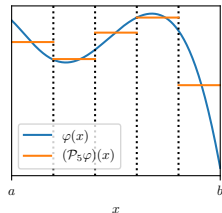
Galerkin method

Example: Ulam's method: $\mathcal{P}_n = L^2$ projection onto piecewise constant functions over even partition of size n .
If f is at least C^2 ,

$$\|\rho_n - \rho\|_{L^2} = \mathcal{O}(n^{-1} \log n).$$

Ulam is a very “low order” method:
basis functions have low regularity, with
consequent slow convergence of solutions
(in low regularity spaces).

In theory of differential equations, etc.
highest-order methods typically use a “spectral” basis of smooth
functions.

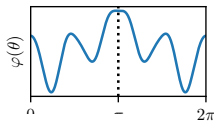


Spectral basis 1: Cosine series

Take an even C^1 function $\varphi : \mathbb{R}/2\pi\mathbb{Z} \rightarrow \mathbb{R}$.

We can write

$$\varphi(\theta) = \sum_{k=0}^{\infty} \hat{\varphi}_k \cos k\theta,$$



where

$$\hat{\varphi}_k = \frac{t_k}{\pi} \int_0^{\pi} \varphi(\theta) \cos k\theta \, d\theta.$$

$t_k = 2 - \delta_{0k}$

Standard result that

$$|\hat{\varphi}_k| = \mathcal{O}(s(k)) := \begin{cases} \mathcal{O}(k^{-r}), & \varphi \in C^r \\ \mathcal{O}(e^{-\delta k}), & \varphi \text{ bd. and analytic} \end{cases}$$

\mathbb{C}
 on $\delta[0, 2\pi]$.

We call $s(\cdot)$ the “spectral” rate of convergence.

Spectral basis 1: Cosine series

We can make the approximation

$$\varphi(\theta) = \sum_{k=0}^{K-1} \hat{\varphi}_k \cos k\theta + \mathcal{O}(K s(K)),$$

where

$$\hat{\varphi}_k = \frac{t_k}{\pi} \int_0^\pi \varphi(\theta) \cos k\theta \, d\theta.$$

Spectral basis 1: Cosine series

We can make the approximation

$$\varphi(\theta) = \sum_{k=0}^{K-1} \hat{\varphi}_k \cos k\theta + \mathcal{O}(Ks(K)),$$

where for $k = 0, \dots, K-1$,

$$\hat{\varphi}_k = \frac{t_k}{K} \sum_{j=0}^{K-1} \varphi(\theta_{j,K}) \cos k\theta_{j,K} + \mathcal{O}(s(K)),$$

where $\theta_{j,K} := \frac{2j+1}{2K}\pi$.

Can compute all K Fourier coefficients with $\mathcal{O}(K \log K)$ operations using FFT algorithm.

Spectral basis 2: Chebyshev series

We can approximate a function

$\psi : [-1, 1] \rightarrow \mathbb{R}$ via cosine series theory

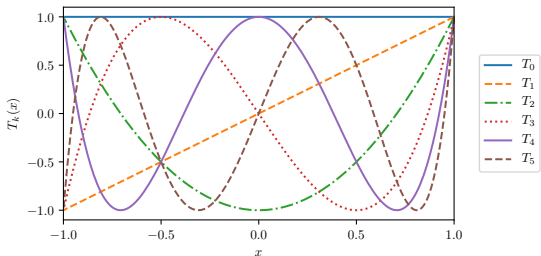
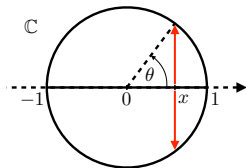
of $\varphi = \psi \circ \cos$.

The Chebyshev polynomials are, for

$x \in [-1, 1]$,

$$T_k(x) = \cos(k \cos^{-1} x).$$

They are orthogonal with respect to the weight $(1 - x^2)^{-1/2}$.



Spectral basis 2: Chebyshev series

Take a C^1 function $\psi : [-1, 1] \rightarrow \mathbb{R}$.

We can write

$$\psi(x) = \sum_{k=0}^{\infty} \check{\psi}_k T_k(x),$$

where

$$\check{\psi}_k = \frac{t_k}{\pi} \int_{-1}^1 \psi(x) T_k(x) \frac{dx}{\sqrt{1-x^2}}.$$

$t_k = 2 - \delta_{0k}$

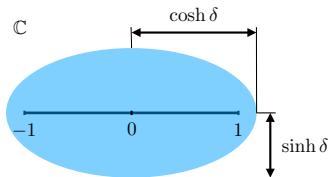
←

Have

$$|\check{\psi}_k| = \mathcal{O}(s(k)) := \begin{cases} \mathcal{O}(k^{-r}), & \psi \in C^r \\ \mathcal{O}(e^{-\delta k}), & \psi \text{ bd. and analytic on } \mathbb{C} \\ & e^\delta\text{-Bernstein ellipse } \overline{-1, 1}. \end{cases}$$

Spectral basis 2: Chebyshev series

A Bernstein ellipse of parameter e^δ is $\cos \delta [0, 2\pi]$:



Spectral basis 2: Chebyshev series

We can make the approximation

$$\psi(x) = \sum_{k=0}^{K-1} \check{\psi}_k T_k(x) + \mathcal{O}(K^{-s(K)}),$$

where

$$\check{\psi}_k = \frac{t_k}{\pi} \int_{-1}^1 \psi(x) T_k(x) \frac{dx}{\sqrt{1-x^2}}.$$

Spectral basis 2: Chebyshev series

We can make the approximation

$$\psi(x) = \sum_{k=0}^{K-1} \check{\psi}_k T_k(x) + \mathcal{O}(K s(K)),$$

where

$$\check{\psi}_k = \frac{t_k}{K} \sum_{j=0}^{K-1} \psi(x_{j,K}) \cos kx_{j,K} + \mathcal{O}(s(K)),$$

where $x_{j,K} := \cos \theta_{j,K} = \cos \frac{2j+1}{2K} \pi$ are the Chebyshev points of the first kind.

Can compute all K Chebyshev coefficients with $\mathcal{O}(K \log K)$ operations using FFT algorithm.

Transfer operator discretisation

Choose projection \mathcal{P}_n to be projection onto first n Chebyshev coefficients, i.e.

$$\mathcal{P}_n \psi = \sum_{k=0}^{n-1} \check{\psi}_k T_k.$$

Then, if $\psi \in \text{im } \mathcal{P}_n$,

$$\mathcal{P}_n \mathcal{L} \psi = \sum_{j=0}^{n-1} \sum_{k=0}^{n-1} \mathcal{L}_{jk} \check{\psi}_k T_j$$

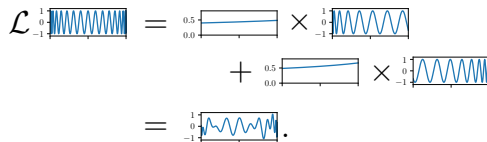
where \mathcal{L}_{jk} is the j th Chebyshev coefficient of $\mathcal{L} T_k$ (computable!).

Discretisation error

The transfer operator sends oscillating functions to functions of lower frequency:

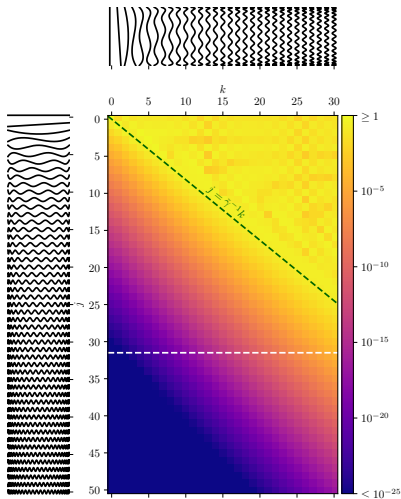
$$\mathcal{L}T_k = \sum_{i \in I} (\sigma_i v_i') \times (T_k \circ v_i).$$

Graphically,



Discretisation error

“Heat map” of $|\mathcal{L}_{jk}|$:



Convergence: bounds on $|\mathcal{L}_{jk}|$

$$\begin{aligned}
 \mathcal{L}_{jk} &= \frac{t_j}{\pi} \int_{-1}^1 (\mathcal{L} T_k)(x) T_j(x) \frac{dx}{\sqrt{1-x^2}} \\
 &= \frac{t_j}{2\pi} \int_0^{2\pi} (\mathcal{L} T_k)(\cos \theta) \cos j\theta \, d\theta \\
 &= \frac{t_j}{2\pi} \sum_{i \in I} \int_0^{2\pi} \underbrace{\sigma_i v_i'(\cos \theta)}_{h_i(\theta)} \cos k \underbrace{(\cos^{-1} v_i(\cos \theta))}_{w_i(\theta)} \cos j\theta \, d\theta \\
 &= \frac{t_j}{2\pi} \sum_{i \in I} \frac{1}{4} \sum_{\pm_1, \pm_2} \int_0^{2\pi} h_i(\theta) e^{i(\pm_1 k w_i(\theta) \pm 2j\theta)} d\theta
 \end{aligned}$$

periodic integral
nice
oscillatory

h_i can be general: could treat Baladi-style weighted transfer operators.

Convergence: bounds on $|\mathcal{L}_{jk}|$

Let's suppose that v_i is analytic on a δ -Bernstein ellipse. Then h_i, w_i are analytic on a complex strip of half-width δ .

We can move the contour of integration by $i\delta$:

$$\begin{aligned} & \int_0^{2\pi} h_i(\theta) e^{i(kw_i(\theta) - j\theta)} d\theta \\ &= \int_0^{2\pi} h_i(\theta + i\delta) e^{ikw_i(\theta + i\delta) - ij(\theta + i\delta)} d\theta \\ &= \int_0^{2\pi} h_i(\theta + i\delta) e^{i(w_i(\theta)k - j\delta) - \delta(j - w_i'(\theta)k) + k\mathcal{O}(\delta^2)} d\theta \end{aligned}$$

So

$$\left| \int_0^{2\pi} h_i(\theta) e^{i(kw_i(\theta) - j\theta)} d\theta \right| \leq \|h_i(\cdot + i\delta)\|_1 e^{-\delta(j - \gamma^{-1}k) + \mathcal{O}(k\delta^2)}$$

Convergence: bounds on $|\mathcal{L}_{jk}|$

Theorem (W. '19)

For all $p > \check{\gamma}^{-1}$ there exists C such that

$$|\mathcal{L}_{jk}| \leq C \min\{1, s(j - pk)\},$$

where s is the spectral convergence rate.

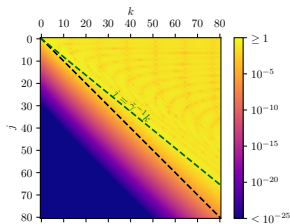


Figure: Heat map of $|\mathcal{L}_{jk}|$ for the Lanford map

Solution operator

We will find estimates for acim, diffusion coefficient, etc. using *solution operator*:

$$\mathcal{S} = (\text{id} - \mathcal{L} + 1_{\mathcal{S}})^{-1}$$

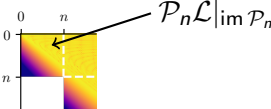
resolvent of \mathcal{L} rank 1 perturbation with left eig'f'n \mathcal{S}

Has useful properties:

- $\mathcal{S}1 = \rho$
- $\mathcal{S}\varphi = \sum_{k=0}^{\infty} \mathcal{L}^k \varphi$ if $\int_{-1}^1 \varphi \, dx = 0$
 - Hence $\sigma_f^2(A) = \mathcal{S} [A(2\mathcal{S} - \text{id})(\rho A - \rho \mathcal{S}[\rho A])]$

Convergence of estimates: operator error

The solution operator is a simple matrix function of \mathcal{L} . We use near-upper-triangularity of \mathcal{L} in Chebyshev basis, computing with:

$$\tilde{\mathcal{L}}_n := \mathcal{L} - (\text{id} - \mathcal{P}_n)\mathcal{L}\mathcal{P}_n =$$


The diagram shows a square matrix with a color gradient from blue (low values) to yellow (high values). The upper triangular part, from row 0 to n and column 0 to n, is yellow. The lower triangular part, from row n to the bottom and column 0 to n, is blue. Dashed lines indicate the boundaries at index n on both axes. An arrow points from the label $\mathcal{P}_n \mathcal{L}|_{\text{im } \mathcal{P}_n}$ to the yellow upper triangular region.

For Banach space \mathcal{B} (e.g. BV) and $\epsilon < 1$ depending on \mathcal{B} , standard relationships between norms and Chebyshev coefficients give

$$\|\tilde{\mathcal{L}}_n - \mathcal{L}\|_{\mathcal{B}} = \left\| \begin{array}{c} 0 \quad n \\ 0 \quad \text{---} \\ n \quad \text{---} \end{array} \begin{array}{c} \text{yellow block} \\ \text{blue block} \end{array} \right\|_{\mathcal{B}} = \mathcal{O}(n^{1+\epsilon} s(n)).$$

The diagram inside the norm is a simplified version of the matrix diagram above, showing the yellow and blue blocks with axes labeled 0 and n.

Convergence of estimates: operator error

Then, since \mathcal{S} is just an operator function of $1_{\mathcal{S}}$ (which is upper-triangular) and \mathcal{L} , if

$$\tilde{\mathcal{S}}_n := (\text{id} - \tilde{\mathcal{L}}_n + 1_{\mathcal{S}})^{-1}$$

then

$$\|\tilde{\mathcal{S}}_n - \mathcal{S}\|_{\mathcal{B}} = \mathcal{O}(n^{1+\epsilon} s(n)),$$

and by block-upper-triangularity we can compute

$$\tilde{\mathcal{S}}_n|_{\text{im } \mathcal{P}_n} = (\text{id} - \mathcal{L}_n + 1_{\mathcal{S}}|_{\text{im } \mathcal{P}_n})^{-1}.$$

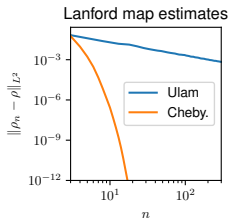
(NB: also possible to use bounds on $|\mathcal{L}_{jk}|$ for estimates in the style of Keller and Liverani '99.)

Computational complexity

Complexity of spectral Galerkin method:

- $n \times \mathcal{O}(n \log n)$
for computation of $\mathcal{P}_n \mathcal{L}|_{\text{im } \mathcal{P}_n}$, plus
- $\mathcal{O}(n^3)$ for matrix
inversion to get solution operator is

$\mathcal{O}(n^3)$ complexity overall, vs $\mathcal{O}(n^{1+\epsilon} s(n))$
decay in error.



Method	Error	Complexity	Error vs Cxty C
Ulam	$\mathcal{O}(n^{-1} \log n)$	$\mathcal{O}(n)$	$\mathcal{O}(C^{-1} \log C)$
Dynamical zeta	$\mathcal{O}(e^{-kn^2})$	$ I ^n$	$\mathcal{O}(e^{-k'(\log I C)^2})$
Chebyshev	$\mathcal{O}(e^{-\delta n})$	$\mathcal{O}(n^3)$	$\mathcal{O}(e^{-\delta' C^{1/3}})$

Table: Comparison of error vs complexity for an analytic map

Poltergeist.jl

Software package written in Julia that uses *adaptive-order* Chebyshev (and Fourier) Galerkin methods to compute statistical properties.

```
[julia> using Poltergeist, ApproxFun]

[julia> A = Fun(x->x^2,0.0..1.0) # functions are approximated as 'Funs'
      Fun(Chebyshev(0.0..1.0),[0.375, 0.5, 0.125])

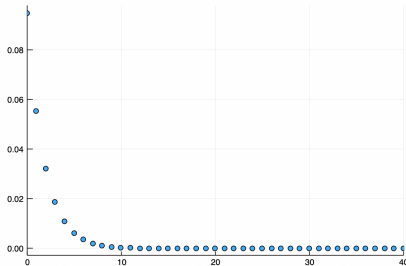
[julia> lanford = modulomap(x->2x+x*(1-x)/2,0.0..1.0)
      MarkovMap 0.0..1.0 → 0.0..1.0 with 2 branches

[julia> L = Transfer(lanford)
      CachedOperator : Chebyshev(0.0..1.0) → Chebyshev(0.0..1.0)
      1.0045576876022717      0.018230750409086872      ...      -0.11314609383584001      ...
      0.1316684582640518      0.5266738330562073      ...      -0.10870638179928527      ...
      0.013630206449799351      0.054520825799197474      ...      -0.32581774878619435      ...
      0.0016352485384284832      0.006540994153714011      ...      0.047971755978939705      ...
      0.0002125058970416101      0.0008500235881663991      ...      -0.1716273579552732      ...
      2.9022773481041993e-5      0.00011609109392424459      ...      0.22837932763765162      ...
      4.094991428494383e-6      1.6379965713883478e-5      ...      0.16173854758342135      ...
      5.906536576252858e-7      2.362614630552166e-6      ...      0.32220668844414624      ...
      8.650893019720111e-8      3.460357204282739e-7      ...      0.13713910992310985      ...
      1.2809804145791083e-8      5.123921654851547e-8      ...      0.04128910954214535      ...
      ...                        ...                        ...                        ...

[julia> @time p = acim(L)
      0.297052 seconds (594.27 k allocations: 29.067 MiB, 1.57% gc time)
      Fun(Chebyshev(0.0..1.0),[1.01524, 0.29594, 0.0454783, 0.00726774, 0.00119289, 0.
      000199207, 3.36268e-5, 5.71372e-6, 9.74689e-7, 1.66662e-7 ... 2.46504e-11, 4.071
      35e-12, 6.73066e-13, 1.11325e-13, 1.8383e-14, 3.02673e-15, 4.96306e-16, 8.09087e
      -17, 1.31132e-17, -2.12448e-18])
```

Poltergeist.jl

```
[julia> lyapunov(L) ]  
0.6576617800065931  
  
[julia> birkhoffvar(L,A) # diffusion coefficient ]  
0.36010948619915506  
  
[julia> scatter(0:40,covariancefunction(L,A,40),xlim=(0,40),legend=false) ]
```



More examples: <https://github.com/wormell/Poltergeist.jl>

Validated bounds

A dramatic example of validated bounds (Theorem 2.5, W. '19):

- a The Lanford map's Lyapunov exponent $L_{exp} := \int_{\Lambda} \log |f'| \rho \, dx$ lies in the range

$$L_{exp} = 0.657\,661\,780\,006\,597\,677\,541\,582\,413\,823\,832\,065\,743\,241\,069\,580\,012\,201\,953\,952\,802\,691\,632\,666\,111\,554\,023\,759\,556\,459\,752\,915\,174\,829\,642\,156\,331\,798\,026\,301\,488\,594\,89 \pm 2 \times 10^{-128}.$$

- b The diffusion coefficient for the Lanford map with observable $A(x) = x^2$ lies in the range

$$\sigma_f^2(A) = 0.360\,109\,486\,199\,160\,672\,898\,824\,186\,828\,576\,749\,241\,669\,997\,797\,228\,864\,358\,977\,865\,838\,174\,403\,103\,617\,477\,981\,402\,783\,211\,083\,646\,769\,039\,410\,848\,031\,999\,960\,664\,7 \pm 6 \times 10^{-124}.$$

These results were obtained in 9 hours on a research server (mostly computing \mathcal{S} , which is reusable).

Application: Pomeau-Manneville systems

Interested in statistical properties
of *non*-uniformly expanding maps

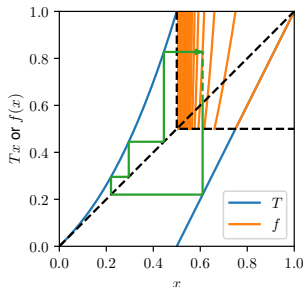
$$T : [0, 1] \rightarrow [0, 1]$$

$$T x = \begin{cases} x(1 + 2^\alpha x^\alpha), & x \leq \frac{1}{2}, \\ 2x - 1, & x > \frac{1}{2}, \end{cases}$$

where $\alpha > 0$.

For example, absolutely continuous
invariant measures: for $\alpha \geq 1$ this
is infinite ergodic theory.

- Lack of uniform expansion and weak mixing properties makes numerics very challenging.
- Ulam-style methods very slow, non-viable for α much greater than 1.



Application: Pomeau-Manneville systems

We approach via induced map

$$f : [\tfrac{1}{2}, 1] \rightarrow [\tfrac{1}{2}, 1]:$$

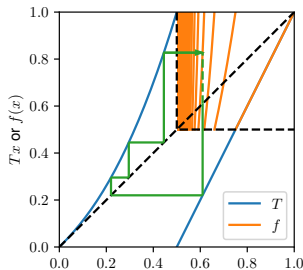
$$f(x) := T^{\tau_T(x)} x.$$

This map is analytic and full-branch uniformly-expanding: we can use Chebyshev methods on it.

Theorem (W., forthcoming)

There exists a real-analytic function $A : (0, 1] \rightarrow [0, \infty)$ such that

$$f(x) = A^{-1}(A(x) \mod 1),$$



Application: Pomeau-Manneville systems

The transfer operator of f is

$$(\mathcal{L}_f \varphi)(x) = \sum_{n=0}^{\infty} \frac{A'(x)}{2} \frac{\varphi(A^{-1}(A(2x-1) + n))}{A'(A^{-1}(A(2x-1) + n))}.$$

Problem: the terms in the sum decay very slowly!

Solution: use smoothness. When $\varphi = T_k$ (i.e. smooth), can use Euler-Maclaurin formula to accurately evaluate $(\mathcal{L}_f \varphi)(x)$.

Application: Pomeau-Manneville systems

Effective estimates of statistical properties of both the induced map and the full, non-uniformly expanding map, for a wide range of α :

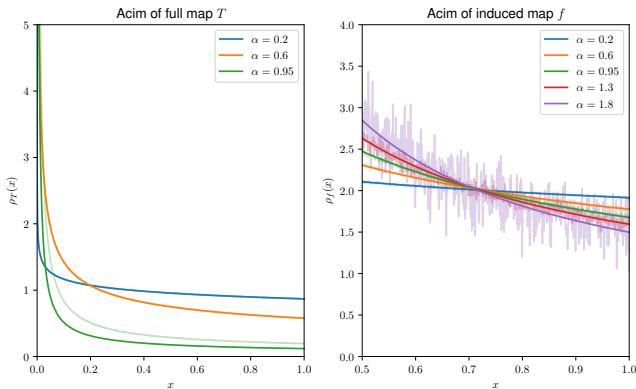


Figure: Acims of the full map with different normalisations. Pale colours indicate estimates from binning on 10^8 simulations.

Application: Pomeau-Manneville systems

Very accurate validated bounds again possible.

For example, the expected return time to $[1/2, 1]$ for $\alpha = 0.95$ (a near-singular case) lies in the range

$$\mathbb{E}_f[\tau_T] = 14.073\ 323\ 220\ 001\ 939\ 529\ 241\ 549\ 699\ 610\ 756\ 609\ 803\ 3171 \pm 10^{-43}.$$

Application: Chaotic hypothesis

Joint work with Georg Gottwald

Chaotic hypothesis (Gallavotti-Cohen)

The macroscopic dynamics of a (high-dimensional) chaotic system on its attractor can be regarded as a transitive hyperbolic (“Anosov”) evolution.

- We derive a “thermodynamic” limiting system of a large self-coupled ensemble of uniformly-expanding maps.
- We use Poltergeist to discover non-hyperbolic dynamics in the limiting system.

Application: Chaotic hypothesis

Consider an ensemble of $M \gg 1$ microscopic constituents $q^{(j)} \in [-1, 1]$ with uniformly expanding dynamics:

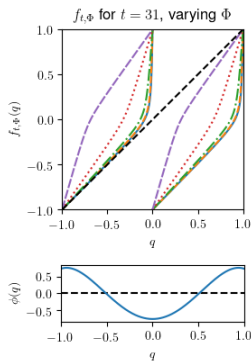
$$q_{n+1}^{(j)} = f_{t, \Phi}(q_n^{(j)}), \quad j = 1, \dots, M.$$

The mean-field

$$\Phi_n = \frac{1}{M} \sum_{j=0}^{\infty} \phi(q_n^{(j)})$$

feeds back into the $q^{(j)}$.

External parameter t which regulates the strength of the feedback.



Application: Chaotic hypothesis

Let $\mu_n(q) \, dq$ be the empirical measure of the $q_n^{(j)}$. Then:

- Dynamics can be formulated

$$\mu_{n+1} = F_t(\mu_n) := \mathcal{L}_{t; \int \phi \mu_n \, dq} \mu_n$$

where $\mathcal{L}_{t; \phi}$ is the transfer operator of $f_{t; \phi}$.

- Mean-field observables (i.e. “macroscopic” dynamics) are expectations over $\mu_n(q) \, dq$;
- In “thermodynamic” limit $M \rightarrow \infty$ reasonable to take $\mu_0 \in C^1$
 \implies **can study dynamics with Chebyshev methods.**

Application: Chaotic hypothesis

The following Poltergeist function iterates μ_n :

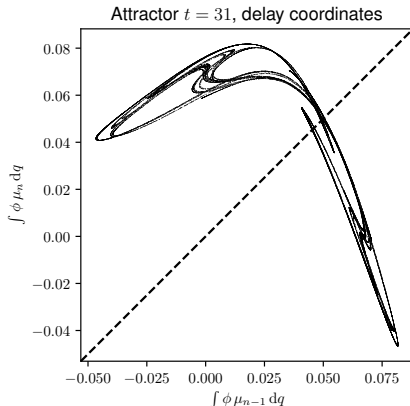
```
function F(mu, t)
    Phi = sum(phi * mu) # 'sum' = total integral
    f = fmap(t,Phi) # predefined initialiser
    return transfer(f,mu)
end
```

For standard double-floating-point implementation this routine evaluates in around 1 millisecond, accurate in norm to $\approx 10^{-13}$.

More details at tinyurl.com/pg-selfcoupled.

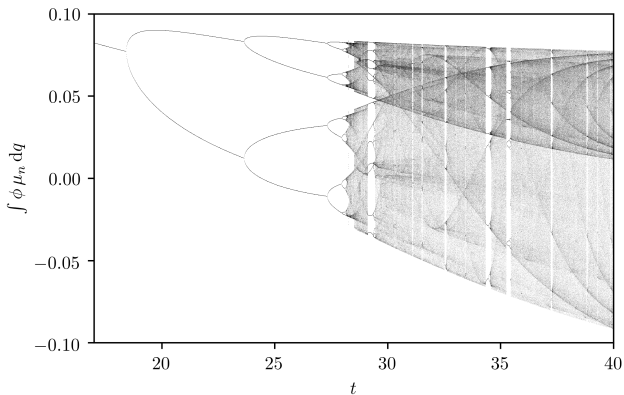
Application: Chaotic hypothesis

- For large t , macroscopic dynamics are chaotic, with quasi-unimodal dynamics in $\Phi_n = \int \phi \mu_n dq$.



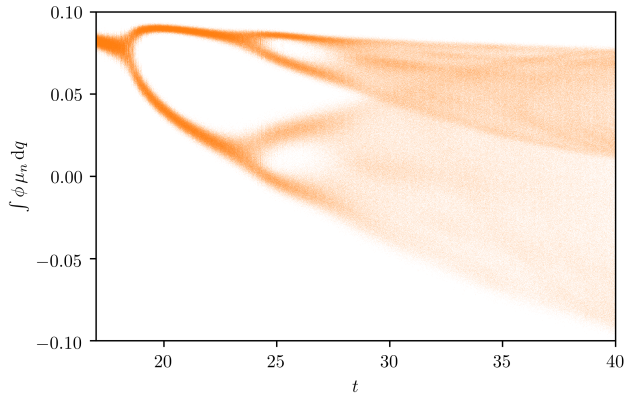
Application: Chaotic hypothesis

Clearly see Henon/logistic-like orbit plot (indicating non-hyperbolicity)



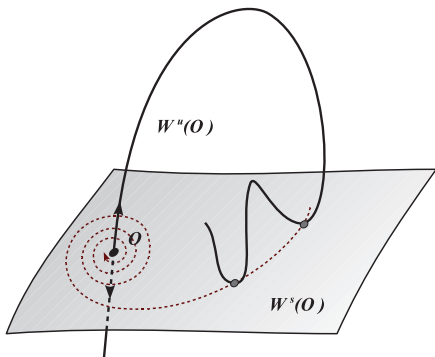
Application: Chaotic hypothesis

Compare with simulations using large, finite $M = 300,000$:



Application: Chaotic hypothesis

Using Poltergeist, we have found direct evidence of non-hyperbolicity in the limit system: a homoclinic tangency.



(Gonchenko *et al*, '12)

Application: Chaotic hypothesis

For $30 \leq t \leq 31$ there is a fixed point $\mu_t^* = F_t(\mu_t^*)$ with $\int \phi \mu_t^* dq \approx 0.05$.

At this fixed point, the Jacobian $J_{\mu_t^*} F_t$ has a single unstable eigenvalue $\lambda_t \sim -1.6$ with (normalised) eigenfunction v_t .

The unstable manifold W_t^u is locally parametrised

$$W_t^u(a) = \mu_t^* + v_t a + \frac{1}{2} h_t a^2 + \mathcal{O}(a^3),$$

with

$$W_t^u(\lambda_t a) = F_t(W_t^u(a)).$$

(Thus, $\{W_t^u(\lambda_t^m a) : m \in \mathbb{Z}\}$ is an orbit originating from μ_t^* .)

Application: Chaotic hypothesis

For a homoclinic, we need the orbit to return to μ_t^* :

$$\lim_{m \rightarrow \infty} W_t^u(\lambda_t^m a) - \mu_t^* = 0 \quad (1)$$

Along the stable manifold, the unstable vector at $W_t^u(a)$ is given by

$$v_{t,a} \propto \frac{d}{da} W_t^u(a) = v_t + h_t a + \mathcal{O}(a^2).$$

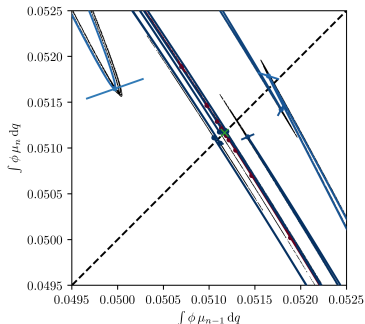
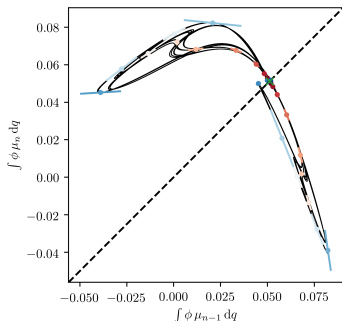
For a stable-unstable tangency $v_{t,a}$ must also be a stable vector, i.e.

$$\lim_{m \rightarrow \infty} J_{F_t^m} W_t^u(a)[v_{t,a}] = 0. \quad (2)$$

Thus, a homoclinic tangency can be found by searching for (a, t) such that (1-2) both hold. We can do this quite efficiently with Poltergeist (as yet no theorems).

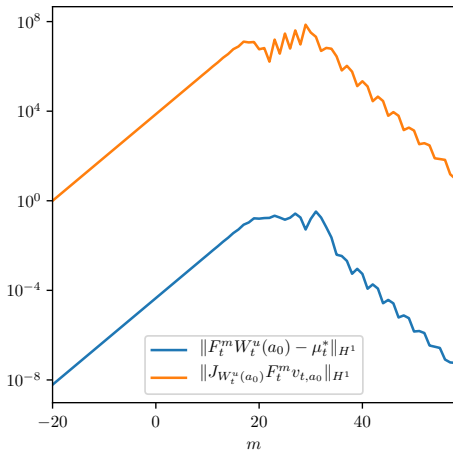
Application: Chaotic hypothesis

Using Poltergeist the following homoclinic tangency was found at $t = 30.0618314$:



Application: Chaotic hypothesis

Error probably of order $\sim 10^{-8}$:



Conclusion

Chebyshev spectral methods:

- Use/respect smooth structure of problem
- Are very efficient
- Are very accurate
- Can be harnessed profitably for study of more complex phenomena in chaotic dynamics.